Contamination by multi step reactions in GEn01

M. Zeier

26th February 2003

We consider multi step reactions which produce uncharged particles that can't be distinguished via "Time of Flight" from neutrons produced by $^2H\,(e,e'n)$ in the target. The following reactions are considered:

- in the lead shielding in front of the neutron detector.
  - $^2H\,(e,e'p)$ followed by $^{208}Pb\,(p,n)$
  - $^2H\,(e,e'p)$ followed by $^{208}Pb\,(p,\pi^0)$ and $\pi^0 \longrightarrow \gamma\gamma$
- in the $^{15}ND_3$ target
  - $^2H\,(e,e'p)$ followed by $^{15}N\,(p,n)$

For the target other materials as ^2H or Al do contribute too, but ^{15}N is the dominant material.

1 $^{208}Pb(p,n)$

A Monte Carlo Simulation has been written to estimate the contamination from (p,n) reactions in front of the neutron detector.

Here the basic layout of the simulation:
Real proton distributions in x and y at bar plane 3 of the neutron detector are taken from the coincidence ntuples after applying the standard cuts on the electron side only. Assuming a straight line for the proton track the interaction point at the lead wall is determined. The proton energy at the Pb plane is calculated from the track time, which is scaled back from third plane to Pb plane assuming constant proton velocity, thus not taking any energy loss into account. Energy loss studies showed that this energy however is accurate to better than 3%.
The energy loss that the proton suffers in the lead is calculated by interpolation from a lookup table containing energy loss for different Pb thickness and impact energies. The proton carries an kinematically dependent asymmetry which is taken from data.

Neutrons are created in the lead wall with angles ϑ (according to $Pb\,(p,n)$ cross section $\times$ phase space) and φ (homogeneous in 2π) and with an energy calculated from relativistic kinematics. If the neutron energy is below the cutoff of the neutron detector the event is discarded.

The neutron detection area is idealized as a homogeneous cube given by the enclosure of all bar planes except the extended top of plane 3. If the neutron vector hits the cube the point of conversion on the neutron track is calculated according to neutron detection efficiency. If the conversion happens within the cube theta_pq, tracktime and ypos of the hit point are calculated and tested for standard cuts. Neutrons that pass are summed up in yield and asymmetry.

In the final calculation an average asymmetry carried by the neutrons is calculated and an effective neutron yield is calculated taking the Pb plane thickness and $Pb\,(p,n)$ cross section into account. The Pb plane has two different thicknesses for the proton part and the neutron part of the detector. A small correction is also done for proton absorbtion in lead.

The contamination is also calculated for the standard binning of theta_np, Eprime, ypos and theta_pq.

Figure 1 shows the content of the setup file that was used to run the simulation for $Q^2 = 0.5$.

1.1 $Pb(p,n)$ cross section

The magnitude of the cross section is adjusted to reproduce results of charge exchange studies for the Basel G_M^n experiment. For that purpose another simulation was written to do the averaging over the extended geometries when it turned out that initial simplified estimates are not accurate enough. The uncertainty of this calibration (7.8%) is given by the accuracy achieved in the G_M^n studies.

The angular dependence of the $Pb\,(p,n)$ cross section is not known but two extreme cases can be assumed:

1. The cross section is purely quasielastic with same angular dependence as free $p-n$ scattering.

2. The cross section is completely flat (phase space only) and the outgoing neutron looses an arbitrary amount of energy.

The simulations are run for these two cases and for the final result the average is taken. The uncertainty of 26.2% is given by the spread of results for the two extreme cases.

1.2 Neutron detection efficiency

The neutron detection efficiency ϵ is given as $\epsilon = 1 - \exp(-\alpha x)$, x being the pathlength and $\alpha = 0.00842\,cm^{-1}$ (according to Glen) derived from an efficiency measurement with a 10cm scintillator bar. The net thickness of all bar planes is 90.4 cm, which gives a neutron detection efficiency of 0.553 for neutrons going

```
### setup file for p-Pb_sim.pl ###
#
# averything after a # is ignored
# format: <variable> = <value>
#

### FLAGS and CUTS ###

#proton asymmetry flag (0=use spline table, 1=use polynomial fit)
#splines recommended, less artefacts in the tails
pAVed_flag = 0

#flags to turn cuts on (1) / off (0)
cut_ypos = 1   #ypos cut
cut_theta_pq = 1 #theta_pq cut
cut_trackt = 1   #tracktime cut

#flag for energy scaling of ndet efficiency:
# ksuvax (1), cross section (0)
ndet_eff_flag = 1

#neutron energy distribution (0=quasielastic, 1=En_lolim..qe)
En_flag = 0

#lower limit of En distribution (only in effect if En_flag=1)
En_ex = 0

#neutron detection energy threshold (MeV)
En_cutoff = 12

### INPUT FILES ###

# np cross section file
cs_file = dsg.dat

# Tables containing energy loss in Pb for different p energy and thickness
elossPb_file = Pb_eloss.dat

# proton asymmetry: file with polinomial fit parameter
pAVed_file = pAVed_fitparam.dat

#proton asymmetry: file with spline curves
pAVed_spline_file = pAVed_thetapq_splines.dat

#input needed for standard binning of kinematic variables
kinvar_scan_file = kinvar_scan.dat

### NDET GEOMETRY ###
#all measures in cm

#distance target to 3rd plane
dist_targ2plane3 = 429.1

#distance lead wall to 3rd plane
dist_Pb2plane3 = 30

#neutron detection area is aproximated as a cube, which is defined by
#the enclosure of all walls in the bar section excluding the top bars
#in plane 3.
length_ndet = 130.7
height_ndet = 172.0
width_ndet = 160

#neutron detection box offset in x
xoff_ndet = 23.2

#Lead wall thickness for lower (neutron) and upper (proton) part
dPb_hi = 1.5
dPb_lo = 2.5

#x position of lead wall thickness change
xPb_dchange = -30.2

### KINEMATICS, EFFICIENCIES, CROSS SECTIONS, ASYMMETRIES ###

#neutron detection efficiency for the length of the detector
ndet_eff_total = 0.533

#The proton efficiency is 0.823 in 25mm Pb and 0.887 in 15mm Pb
p_eff_lo = 0.823
p_eff_hi = 0.887

#ratio 0 deg c.s. Pb(p,n)/p-n:
ratio_cs0 = 26.02

#measured asymmetries butcher v16
asym_p = -0.1547
asym_n = 0.03464

#reference gamma time (ns)
gref_tof = -8.4

#nominal central momentum neutron energy (MeV)
En_nom = 288

#Proton energy correction factor:
#Calculation from TOF underestimates proton energy before Pb wall due to
#energy loss during flight path.
Ep_corrfac = 1.021

#neutron energy subtraction (e.g. Q value)
En_offset = 3.7

### CONSTANTS ###

dens_Pb = 11.35     #Lead density (g/cm^3)
mol_Pb = 208        #Lead molular weight
N_A = 6.0222e23     #Avogadros number(/mol)
m_n = 939.566       #neutron mass (GeV/c^2)
m_p = 938.272       #proton mass (GeV/c^2)
```

Figure 1: Standard configuration for $Pb\,(p,n)$ simulation for $Q^2 = 0.5$

Table 1: List of systematic contributions

Source	rel error (%)
$Pb(p,n)$ cross section	26.2
neutron detection efficiency	7.5
neutron detector geometry	7.4
proton asymmetry from butcher	1.2
proton energy from TOF	0.4
G_M^n CEX uncertainty	7.8
G_M^n CEX simulation: statistics	3.0
Main simulation: statistics	1.5
Total	29.5

through the full length of the detector. In the simulation we use an homogeneous neutron detection cube instead of scintillator walls. In this idealization the detection material is diluted and α is adjusted accordingly. The detection probability at pathlength x for a single neutron is given as $\exp(-\alpha x)$. Assuming an error of 10% in α results in a 7% error in the contamination.

For the energy dependence of the neutron detection efficiency KSUVAX was run by Glen for different neutron energies. The efficiency remains constant within 10% down to about 55MeV and falls off rapidly below. α is scaled accordingly. Repeating the simulation with a completely flat efficiency reveals a difference of 2.7% in contamination.

1.3 Transferred Asymmetry

The neutrons produced by $Pb\,(p,n)$ carry the asymmetry of the proton. To determine the size of that asymmetry transfer we used measured proton asymmetries as a function of *theta_pq* and *ypos*. The *theta_pq* dependence of the asymmetry for different ypos bins was interpolated using weighted splines as shown in figure 2. The proton asymmetries have standard cuts on the electron side applied and were obtained from Frank who ran a customized "butcher" for that purpose. The error involved here is simply given by the statistical uncertainty of the proton asymmetries (1.2%).

1.4 Results

The contamination for $Q^2 = 0.5$ is in the order of 3-4% and can be determined with an accuracy of 1% absolute. The latest numbers are found on the web page.

Figures 3 and 4 show distributions generated by the simulation.

Table **??** lists contributions to the systematic error.

The simulation was not run for $Q^2 = 1$ but a simple estimate indicates that the contamination is about the same as for $Q^2 = 0.5$.

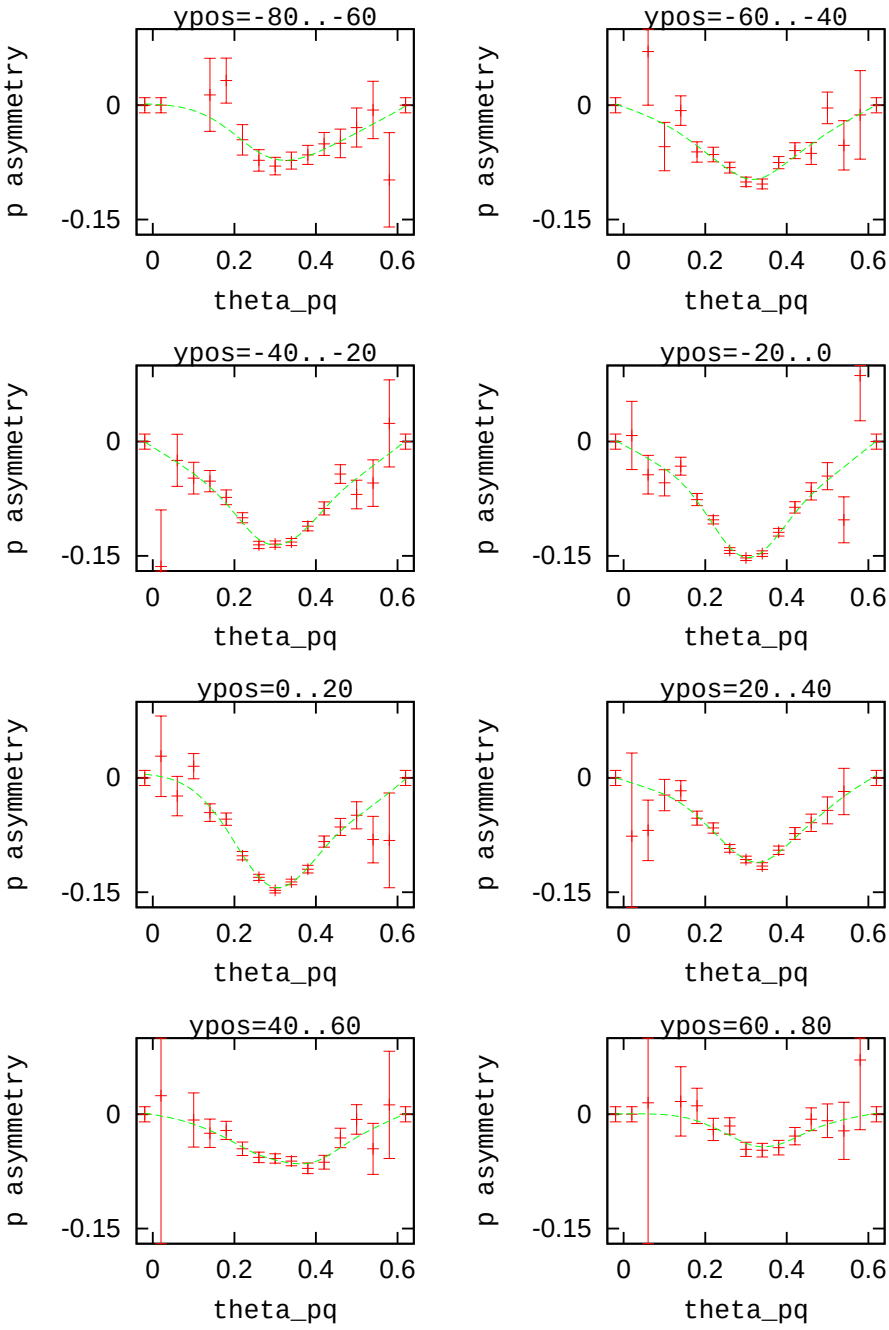

Figure 2: Proton asymmetries vs. theta_pq for different ypos bins. The lines are weighted splines.

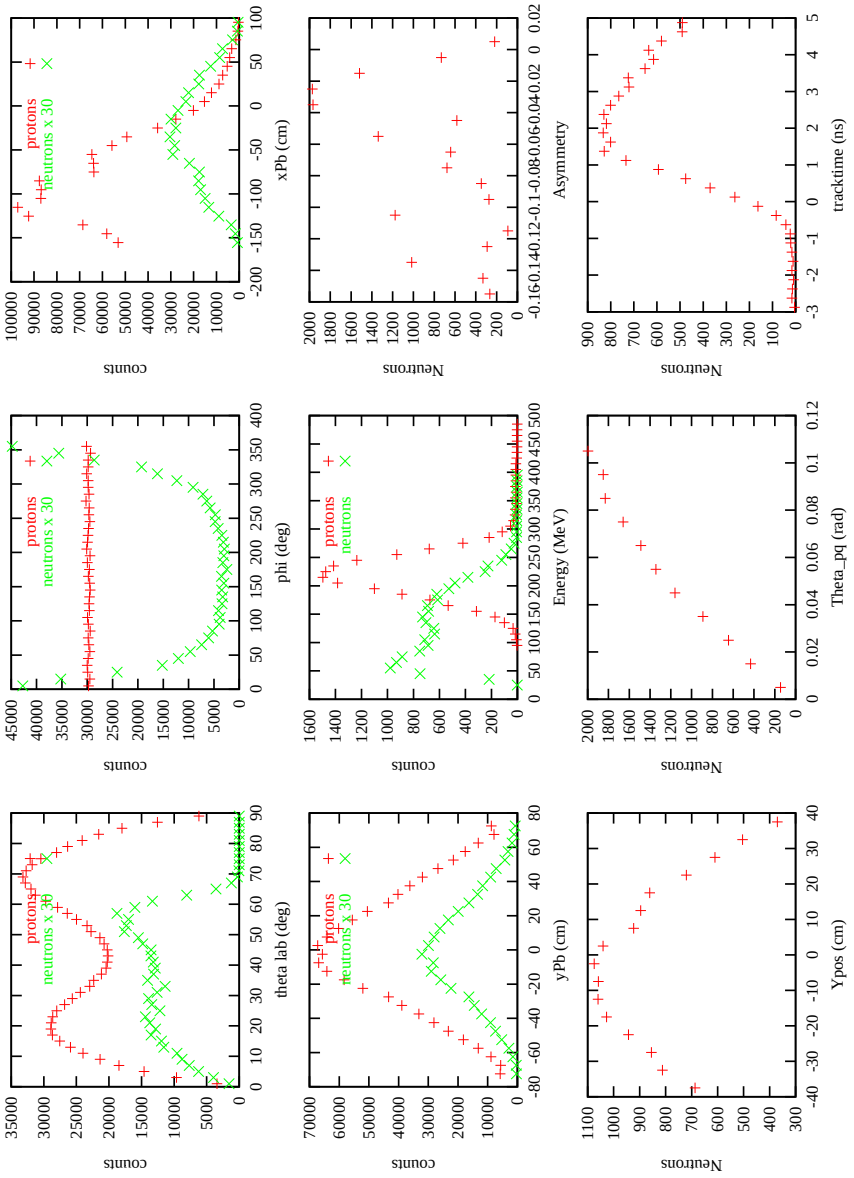

Figure 3: $Q^2 = 0.5$ distributions for the quasielastic case. The following variables are plotted: neutron angles (*theta_lab*, *phi*) before (*proton*) and after (*neutron*) cuts, proton distribution on lead wall (*xPb*,*yPb*) before (*proton*) and after (*neutron*) cuts, proton energy and neutron energy both after cuts and asymmetry and kinematic variables (*Ypos*, *Theta_pq* and *tracktime*) of neutrons after cuts. Cuts applied are std cuts as defined in the "butcher".

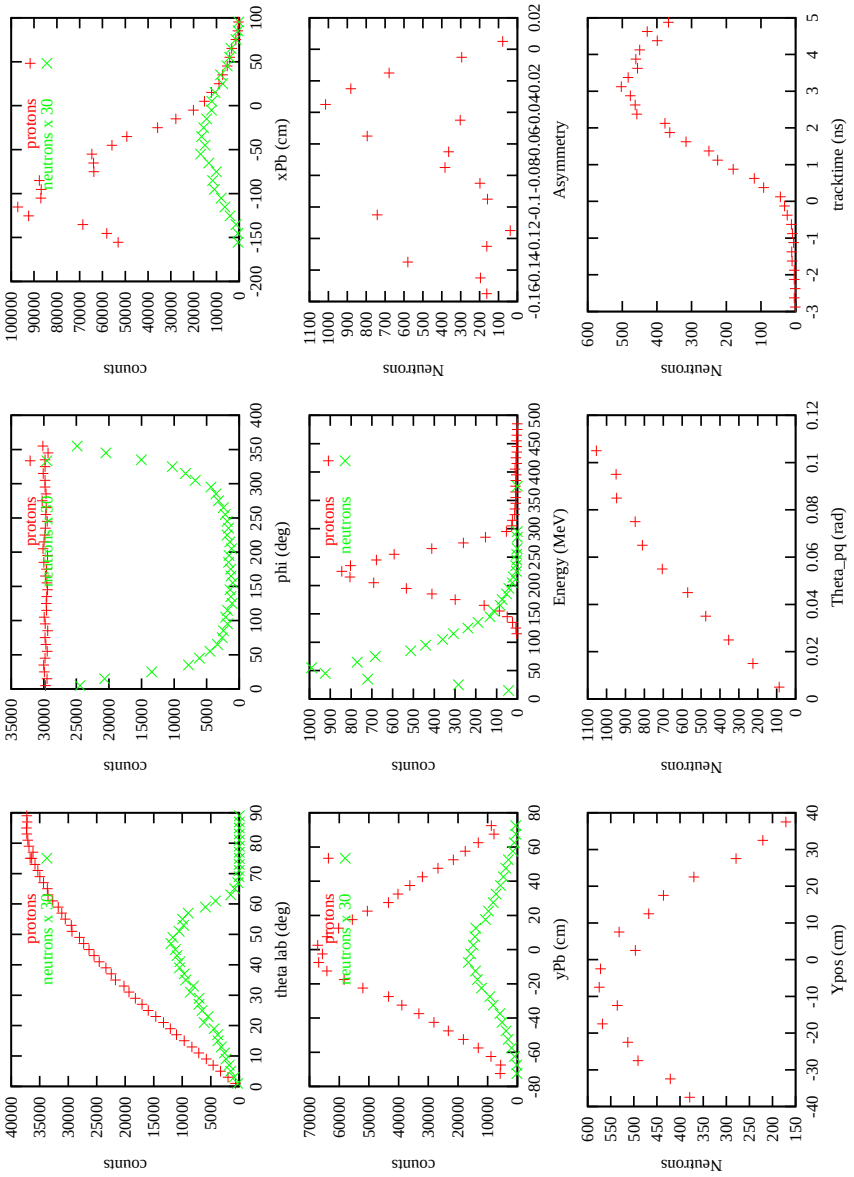

Figure 4: Same as figure 3 but for the flat case.

2 $^{15}N(p,n)$

A quick estimate was done based on the following:

- proton and neutron yields and asymmetries based on "butcher" results.
- average path of proton in target based on geometry
- $^{15}N(p,n)$ cross section scaled with $A^{\frac{2}{3}}$ from $^{208}Pb(p,n)$.
- average solid angle based on neutron detector geometry

The contamination is estimated to be small (0.3%).

3 Photon contamination

Total cross sections for $p-p \rightarrow \pi^0$ at our proton energies have been measured by Meyer et al (NPA539, 633, 1992 and PRL65, 2846, 1990) and by Stallwood et al (PR109, 1710, 1958). The latter also measured $p-Pb \rightarrow \pi^0$ total cross section at 425 MeV proton energy.

The $p-p$ cross section shows a sharp increase from <1 μbarn at 270 MeV ($Q^2=0.5$) to 1 mbarn at 530 MeV ($Q^2=1$). Scaling the $p-Pb$ cross section accordingly gives a total cross section of 0.1 mbarn for $Q^2=0.5$ and 100 mbarn at $Q^2=1$. This needs to be compared to a total $Pb(p,n)$ cross section which is in the order of 1000 mbarn.

For $Q^2=0.5$ the effect is neglible while for $Q^2=1$ it is still small even if one considers that the photon detection efficiency of the neutron detector is about 40% larger than the neutron detection efficiency.